FRIGID ZONE **MEDICINE**
Original Article • DOI: 10.1515/fzm-2025-0022

Circular RNA signatures in vestibular migraine and migraine from cold regions: Preliminary mechanistic insights

Qihui Chen[1,2,3], Jinghan Lin[1,2], Qingling Zhai[1,2,4], Qijun Yu[1,2,4], Yonghui Pan[1,2*]

Abstract

Background: Vestibular migraine (VM) is a common disorder characterized by recurrent dizziness or vertigo, often aggravated by cold exposure. This study aimed to identify differentially expressed circular RNAs (circRNAs) in cold-region VM and explore the underlying molecular mechanisms. **Methods:** Peripheral blood samples from long-term residents of Heilongjiang Province profiled by circRNA microarray, and differentially expressed circRNAs were validated by quantitative reverse transcription polymerase chain reaction (qRT-PCR). A competing endogenous RNA (ceRNA) network and enriched pathways were inferred by bioinformatics. A VM-like mouse model was established using nitroglycerin (NTG) and kainic acid (KA) and confirmed by behavioral testing and western blot. The hsa_circ_0003201/miR-31-5p/triggering receptor expressed on myeloid cells 2 (TREM2) axis and related pathways were examined in clinical samples and in the trigeminal nucleus caudalis (TNC) and vestibular nuclei (VN) of mice using qRT-PCR, enzyme-linked immunosorbent assay (ELISA), and western blot. CircRNA microarray profiling also compared expression patterns between VM and migraine patients. **Results:** Hsa_circ_0003201 was significantly upregulated in cold-region VM patients. Bioinformatic analyses revealed that hsa_circ_0003201 may regulate the miR-31-5p/TREM2 axis and be associated with phosphoinositide 3-kinase (PI3K)/protein kinase B (AKT) signaling, pyruvate metabolism, and transient receptor potential (TRP) pathways. Clinical validation confirmed increased hsa_circ_0003201 and TREM2 and decreased miR-31-5p. VM-like mice exhibited central sensitization and vestibular dysfunction, with increased TREM2, decreased miR-31-5p, and PI3K/AKT activation in the TNC and VN. Comparative circRNA analysis between VM and migraine patients indicated distinct expression patterns. **Conclusion:** Hsa_circ_0003201 shows potential as a diagnostic biomarker for cold-region VM, and the hsa_circ_0003201/miR-31-5p/TREM2 axis may contribute to pathogenesis through PI3K/AKT signaling, pyruvate metabolism, and TRP-related pathways.

Keywords

circRNA; vestibular migraine; cold regions

Received 16 September 2025, accepted 08 October 2025

[1]*Harbin Medical University, Harbin 150081, China*
[2]*Department of Neurology, The First Affiliated Hospital of Harbin Medical University, Harbin 150001, China*
[3]*Key Laboratory of Hepatosplenic Surgery, Ministry of Education, The First Affiliated Hospital of Harbin Medical University, Harbin 150001, China*
[4]*NHC Key Laboratory of Cell Transplantation, The First Affiliated Hospital of Harbin Medical University, Harbin 150001, China*

**Corresponding authors Yonghui Pan, E-mail: aigui1993@126.com*

1 Introduction

Migraine (M) is a common chronic neurovascular disorder with a global prevalence of approximately 10%[1] and the second leading cause of disability among neurological diseases[2]. Vestibular migraine (VM), a migraine-related central nervous system disorder, is characterized by recurrent vertigo or dizziness, imbalance, and spatial disorientation, with or without headache. Its annual prevalence is ~2.7% in the general population[3], and moderate-to-severe vestibular symptoms substantially impair daily and social functioning. Environmental factors, particularly temperature change, are recognized triggers for both M and VM[4-5]. Li *et al.* reported greater susceptibility to headaches during sudden temperature drops or cold exposure[6], and a separate study found that a 5 °C decrease in mean temperature 1-3 days prior was

associated with a 24% ± 8% increase in migraine-related messages[7]. These observations implicate cold stimulation in the onset and progression of M and VM. Populations living in cold regions show higher prevalence of these disorders, potentially reflecting more complex pathophysiology. Clarifying the molecular mechanisms of M and VM in cold regions is therefore essential for pathogenesis, prevention, and region-adapted treatment strategies.

Despite advances, the pathophysiological mechanisms of M and VM remain incompletely understood. Diagnosis still relies largely on clinical criteria and exclusion, and the lack of objective, sensitive biomarkers limits early detection and precision therapy. Circular RNAs (circRNAs) are covalently closed non-coding RNAs generated by back-splicing of pre-mRNAs; they are abundant, stable, and display tissue-specific expression[8]. CircRNAs contribute to disease initiation and progression through multiple mechanisms, including functioning as competing endogenous RNAs (ceRNAs) that modulate microRNA (miRNA) activity, interacting with circRNA-binding proteins (cRBPs), encoding peptides, and regulating transcriptional or post-transcriptional processes[9]. Recent progress in *in vitro* synthesis and targeted delivery has furthered their translational potential[10]. Accordingly, circRNAs are promising candidates for disease diagnosis, prognostication, and targeted therapy. Prior work implicates circRNAs in pain pathogenesis *via* ion-channel modulation, regulation of pro-/anti-inflammatory signaling, and control of transcription factors involved in nociceptor sensitization[11]. Lin *et al.* identified differentially expressed circRNAs in migraine patients[12]. Moreover, in postmortem interval (PMI) mouse models exposed to different temperatures (4 °C, 25 °C, 35 °C), circRNAs displayed greater stability at low temperature[13], suggesting cold-specific expression patterns. Temperature may therefore regulate circRNA abundance, splicing, and functional networks, contributing to adaptive responses to environmental cold—an insight directly relevant to cold-region M and VM.

Heilongjiang Province, a high-latitude cold region of China, provides a natural population base for investigating temperature-related influences on M and VM. In this study, we profiled circRNA expression in peripheral blood from long-term Heilongjiang residents, identified differentially expressed circRNAs in M and VM patients from cold regions, and explored candidate mechanisms and signaling pathways in clinical samples and animal models. We also compared circRNA expression patterns between M and VM to delineate their molecular relationships and to characterize circRNA features specific to cold-region populations.

2 Materials and methods

2.1 Blood sample collection

We enrolled 4 patients with M and 53 with VM from neurology outpatient clinics and inpatient wards. All patients met International Classification of Headache Disorders, 3rd edition (ICHD-3) diagnostic criteria for M without aura and for VM[14]. An additional 53 age- and sex-matched healthy controls were recruited (Table 1). All participants were long-term residents of Heilongjiang Province and had not used acute analgesics or anti-vertigo/dizziness medications within 48 h before enrollment, nor prophylactic treatments within the prior week. The study conformed to the Declaration of Helsinki (1964 and later revisions) and was approved by the institutional ethics committee (IRB-AF/SC-12/03.0). Written informed consent was obtained from all participants.

2.2 Peripheral blood circRNA microarray

Total RNA was isolated from peripheral blood samples of 3 VM patients, 4 M patients, and 3 healthy controls. RNA quantity and purity were assessed spectrophotometrically; acceptable A260/A280 ratios were between 1.8 and 2.1. To enrich circRNAs, linear RNAs were digested with RNase R. The remaining RNAs were amplified and labeled using the Arraystar Super RNA Labeling Kit and purified with the RNeasy Kit. Labeled cRNAs were hybridized to the Arraystar Human circRNA Array V2 and scanned on an Agilent G2505C microarray scanner. Raw images were processed with Agilent Feature Extraction software, followed by quantile normalization and differential-expression analysis using the limma package in R. Differentially expressed circRNAs were determined using volcano-plot visualization and predefined fold-change and significance thresholds.

2.3 Quantitative reverse transcription polymerase chain reaction (qRT-PCR)

For circRNAs, reverse transcription was performed with the ReverTra Ace qPCR RT Kit (TOYOBO, Japan); for miRNAs, the Bulge-Loop™ miRNA qRT-PCR Starter Kit (RiboBio, Guangzhou, China) was used per manufacturers' instructions. qRT-PCR was performed with SYBR Green Master Mix (ROX, USA) and gene-specific primers (Table 2) using the following program: 95 °C for 10 min; 40 cycles of 95 °C for 5 s, 60 °C for

Table 1 Comparison of age and sex among enrolled patients

	Control (*N* = 53)	VM (*N* = 53)	*P* value
Age	52.77 ± 11.84	56.25 ± 10.16	0.1116
Sex			0.5260
Male	7	4	
Female	46	49	

Table 2 Sequences of primers used in quantitative reverse transcription polymerase chain reaction (qRT-PCR)

Name	Sequence
β-actin	F: 5' GTGGCCGAGGACTTTGATTG3' R: 5' CCTGTAACAACGCATCTCATATT3'
hsa_circ_0046435	F: 5' TCTAGGTCAACACCAGCTACCA3' R: 5' GCGGCACTTTGATGAAATAAC3'
hsa_circ_0003201	F: 5' TCTGAAGTGGAGAACGAAGAAAT 3' R: 5' CTTCATACTGCTGTCTGTGCTTC 3'
hsa_circ_0007548	F: 5' CTACTCTCTGCTTCCCTAGACAAC 3' R: 5' TTTGATGTGACGTAAGTTTTTGC 3'
hsa_circ_0028196	F: 5' CCCTTGATGCCATTCTAGTGA 3' R: 5' CACAGCATTCCGATATTCCTT 3'
hsa_circ_0000745	F: 5' TTACTAAAGGCAAACGGTGAA 3' R: 5' GAGTGGGAGTGTTGGAAGAAG 3'
hsa_circ_0002513	F: 5' TCAAAGCTGCCCAATGATCTG 3' R: 5' GGAAAGTGTAGTTGCCCTCCC 3'
hsa_circ_0001965	F: 5' ACCAGTTAATAGCACCAGCTGA 3' R: 5' GACGACGAGACAACAGGAATG 3'
hsa_circ_0001772	F: 5' GAACCTTTAGATGAATTTACATGAA 3' R: 5' CCGACTGATTCTTTTTGCC 3'

hsa-miR-31-5p and mmu-miR-31-5p were designed and synthesized by RiboBio (Guangzhou, China).

20 s, and 72 °C for 10 s. β-actin served as the reference for circRNAs and U6 for miRNAs. All reactions were run in triplicate; relative expression was calculated by the $2^{-\Delta\Delta CT}$ method.

2.4 Enzyme-linked immunosorbent assay (ELISA)

Serum triggering receptor expressed on myeloid cells 2 (TREM2) levels was measured using a human TREM2 ELISA kit (Jianglai, Shanghai, China). Fasting venous blood (3-5 mL) was collected into EDTA tubes, centrifuged at 1000 rpm for 20 min, and supernatants were diluted 1∶1 with PBS. Standards, samples, and blanks (100 μL/well, in triplicate) were incubated at 37 °C for 1 h, followed by 100 μL biotinylated antibody for 1 h. After three washes, 100 μL enzyme conjugate was added for 30 min, plates were washed five times, and 90 μL TMB substrate was added for 15 min at 37 °C in the dark. Reactions were stopped with 50 μL stop solution, and absorbance was read at 450 nm. Concentrations were calculated from the standard curve.

2.5 Animals

All procedures were approved by the Institutional Animal Care and Use Committee (No. 2022-K98). Male C57BL/6J mice (≈25 g) were obtained from Liaoning Changsheng Biotechnology Co., Ltd. Animals were housed under standard conditions (23 ± 1 °C; 12-h light/dark cycle) with ad libitum access to food and water.

2.6 Migraine model

Migraine-like hypersensitivity was induced by intraperitoneal nitroglycerin (NTG, 10 mg/kg; Shandong, China) administered once every two days for five injections over 9 days[15].

2.7 VM model

After M modeling, vestibular injury was induced as described previously. Mice were positioned on a surgical platform and the fur around the ears was removed. Under a dissecting microscope, the tympanic membrane was exposed and perforated with a 30-gauge needle. Then, 10 μL of 12.5 mmol/L kainic acid (KA) was slowly injected into the middle ear[16]. Animals were maintained in the injection position for 30 min to ensure exposure, recovered on a warming pad, and returned to clean cages with free access to food and water. If severe imbalance interfered with feeding or drinking, gelatin was provided as supplemental nutrition and hydration.

2.8 Periorbital mechanical thresholds

Periorbital mechanical sensitivity was assessed with von Frey filaments starting at 0.6 g. Each filament was applied perpendicularly for 3-6 s. Positive responses included asymmetric head withdrawal, avoidance, or defensive behaviors. Withdrawal thresholds were calculated using the up-down method[17].

2.9 Balance beam walk

The balance beam test was performed as previously reported[18]. Briefly, a horizontal beam was placed 40 cm above the ground with a soft cushion underneath. The time to traverse the beam was recorded (cutoff 90 s). Each mouse completed three trials separated by ≥ 5 min. Trials with falls or non-completion were excluded; the mean time of completed trials was analyzed. Values > 60 s were recorded as 60 s.

2.10 Vestibular dysfunction tests

Vestibular dysfunction was evaluated after the fifth modeling session as previously described[19]. Six parameters were scored: head movement, circling, retreat, tail suspension reflex, contact inhibition reflex, and righting reflex in the air. Each item was rated 0-2 (0 = normal, 1 = mild deficit, 2 = severe deficit); the composite score (maximum 12) indexed overall vestibular impairment.

2.11 Western blot (WB)

Brain tissues were homogenized and lysed in RIPA buffer (Seven, Beijing, China) containing phosphatase inhibitors (Rox, USA) and PMSF (Seven, Beijing, China). Protein concentration was determined by spectrophotometry (Gene, Shanghai, China). Samples were mixed with 5×loading buffer (Beyotime, Shanghai, China), denatured at 95 °C for 10 min, separated by SDS-PAGE, and transferred to PVDF membranes. Membranes were blocked with 5% milk, incubated with primary antibodies (Table 3) overnight at

4 °C, followed by secondary antibodies (Table 3) for 1 h at room temperature. Bands were visualized with ECL (Biosharp, USA) and quantified using ImageJ, normalized to the indicated loading controls.

2.12 Statistical analysis

Data were analyzed in GraphPad Prism 9.1.5 and are presented as mean ± SD. Each experiment was performed in at least three independent replicates. Behavioral outcomes were analyzed by two-way ANOVA with Tukey's post-hoc test. Pairwise comparisons used Student's *t*-test; multi-group comparisons used one-way ANOVA. A two-sided $P < 0.05$ was considered statistically significant.

3 Results

3.1 Hsa_circ_0003201 is upregulated in the peripheral blood of VM patients from cold regions

To identify differentially expressed circRNAs in cold-region VM, we performed circRNA microarray profiling on peripheral blood from 3 VM patients and 3 healthy controls. We detected 145 differentially expressed circRNAs (FC ≥ 1.5, $P < 0.05$), including 17 upregulated and 128 downregulated transcripts (Fig. 1A, 1B). The top four up- and top four downregulated circRNAs were prioritized (Fig. 1C); their expression levels and host genes are listed in Table 4. qRT-PCR in the discovery samples confirmed microarray-consistent changes for hsa_circ_0003201, hsa_circ_0028196, hsa_circ_0000745, hsa_circ_0001965, and hsa_circ_0001772 (hsa_circ_0003201: $P = 0.0099$; hsa_circ_0028196: $P = 0.0405$; hsa_circ_0000745: $P = 0.0047$; hsa_circ_0001965: $P = 0.0041$; hsa_circ_0001772: $P = 0.0067$; $N = 3$/group, Student's *t*-test; Fig. 1D, 1E). In an expanded clinical cohort ($N = 20$/group), hsa_circ_0003201 remained significantly upregulated in VM ($P = 0.0002$), whereas hsa_circ_0028196, hsa_circ_0000745, and hsa_circ_0001772 did not show robust between-group differences ($P = 0.3124$; 0.0770; 0.0356, respectively; Student's *t*-test; Fig. 1F). Based on consistency and effect size, hsa_circ_0003201 was selected for follow-up analyses.

Table 3 Antibodies for western blot

Name	Manufacturer	Catalog Number	Dilution
CGRP	Abcam	ab283568	1：1000
c-Fos	CST	2250	1：1000
GAPDH	Immunoway	YN5585	1：10000
TREM2	MCE	HY-P80920	1：1000
β-Actin	Affinity	T0022	1：10000
PI3K	Immunoway	YT6156	1：2000
P-AKT	Immunoway	YP0006	1：2000
AKT	Immunoway	YT0185	1：2000
Goat Anti Rabbit IgG (H+L)	Immunoway	RS0002	1：10000
Goat Anti Mouse IgG (H+L)	ABclonal	AS003	1:10000

CGRP, Calcitonin gene-related peptide; GADPH, glyceraldehyde-3-phosphate dehydrogenase; TREM2, triggering receptor expressed on myeloid cells 2; PI3K, phosphoinositide 3-kinase; AKT, protein kinase B; IgG, immunoglobulin G.

3.2 Differential expression of the hsa_circ_0003201/miR-31-5p/TREM2 axis in VM from cold regions

Gene Ontology (GO) (Fig. 2A) and KEGG enrichment (Fig. 2C) of mRNAs associated with hsa_circ_0003201 indicated links to PI3K/AKT signaling and pyruvate metabolism. Although transient receptor potential (TRP) pathways (hsa04270, hsa04750) did not rank among the top-20 terms, they remain biologically relevant; representative pathway maps are shown in Fig. 2D. Predicted miRNA targets of hsa_circ_0003201 and their downstream mRNAs were integrated into a ceRNA network, from which the hsa_circ_0003201/miR-31-5p/TREM2 axis emerged as a candidate pathway in VM (Fig. 2B). Validation in clinical samples demonstrated higher hsa_circ_0003201 ($P = 0.0002$, $N = 30$/group; Fig. 2E) and TREM2 ($P = 0.0001$; Fig. 2G) and lower miR-31-5p ($P = 0.0159$; Fig. 2F) in VM versus controls (Student's *t*-test). Together, these findings support dysregulation of the hsa_circ_0003201/miR-31-5p/TREM2 axis in cold-region VM and implicate PI3K/AKT, pyruvate metabolism, and TRP-related pathways.

3.3 VM-like mouse models exhibit central sensitization with vestibular impairment

We established a VM-like model by alternate-day intraperitoneal

Table 4 Top 4 upregulated and top 4 downregulated circRNAs in vestibular migraine (VM) patients

Circbase ID	Chrom	*P* value	Fold change (abs)	Regulation	circRNA_type	Gene symbol
hsa_circ_0046435	chr17	0.035982	2.125836	Up	Exonic	FOXK2
hsa_circ_0003201	chr4	0.017203	1.724902	Up	Exonic	TBC1D14
hsa_circ_0007548	chr16	0.013781	1.546976	Up	Exonic	RFWD3
hsa_circ_0028196	chr12	0.024714	1.514584	Up	Exonic	ANAPC7
hsa_circ_0000745	chr17	0.003209	2.660764	Down	Exonic	SPECC1
hsa_circ_0002513	chr11	0.026517	2.612719	Down	Exonic	PICALM
hsa_circ_0001965	chr3	0.040671	2.376915	Down	Exonic	PHC3
hsa_circ_0001772	chr7	0.038666	2.136985	Down	Exonic	RBM33

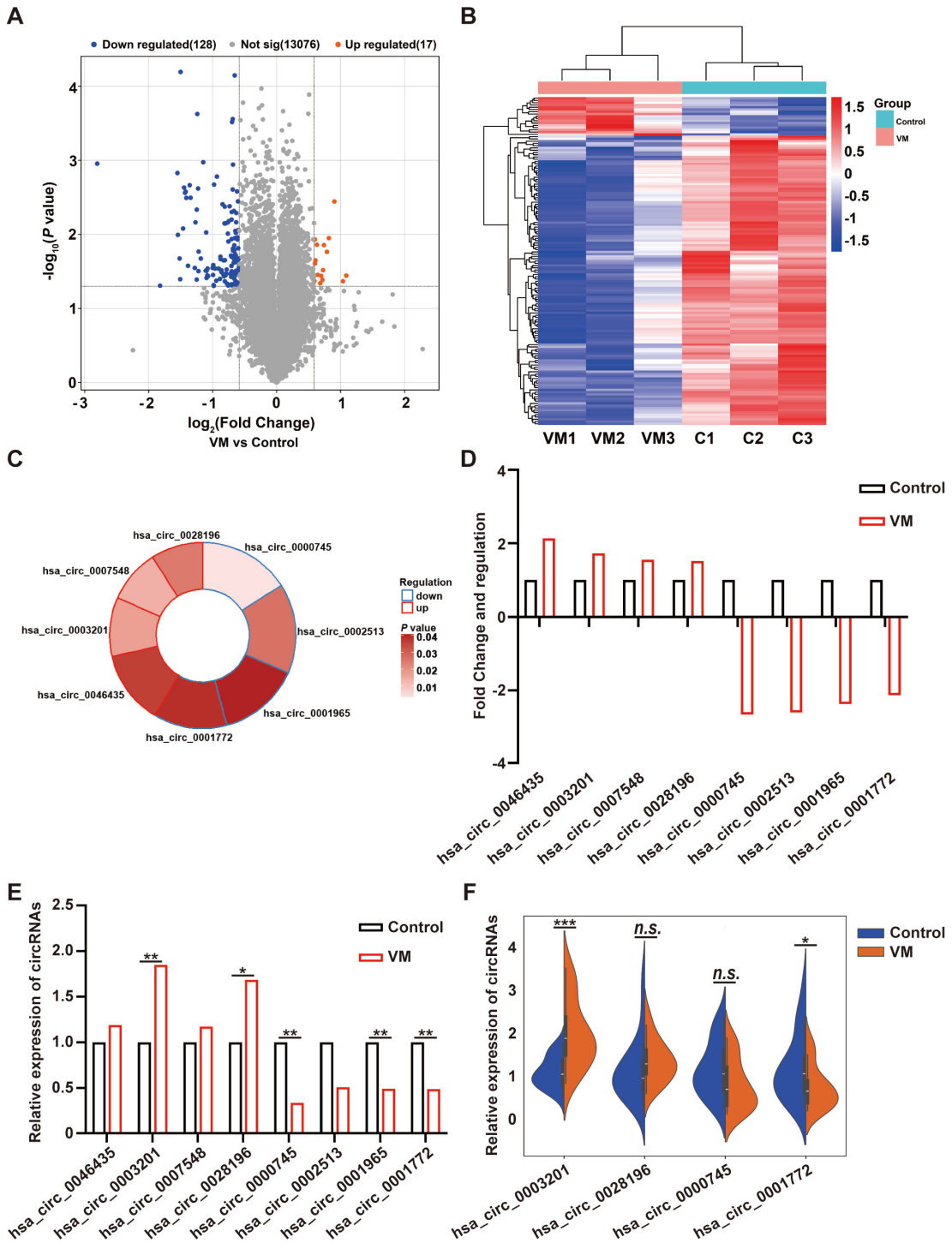

Fig. 1 Screening and validation of differentially expressed circRNAs in vestibular migraine (VM) patients

(A-B) Volcano plot and hierarchical clustering of differentially expressed circRNAs between VM patients and healthy controls. (C) Top 4 upregulated and top 4 downregulated circRNAs. (D) Microarray expression patterns of the 8 candidate circRNAs (N = 3/group). (E) Validation of the 8 candidate circRNAs by quantitative reverse transcription polymerase chain reaction (qRT-PCR) (N = 3/group). (F) Relative expression of the 4 selected circRNAs in VM patients measured by qRT-PCR (N = 20/group). The data are presented as mean ± SD. Student's t-test (E and F). $^{*}P < 0.05$, $^{**}P < 0.01$, $^{***}P < 0.001$. n.s., not significant.

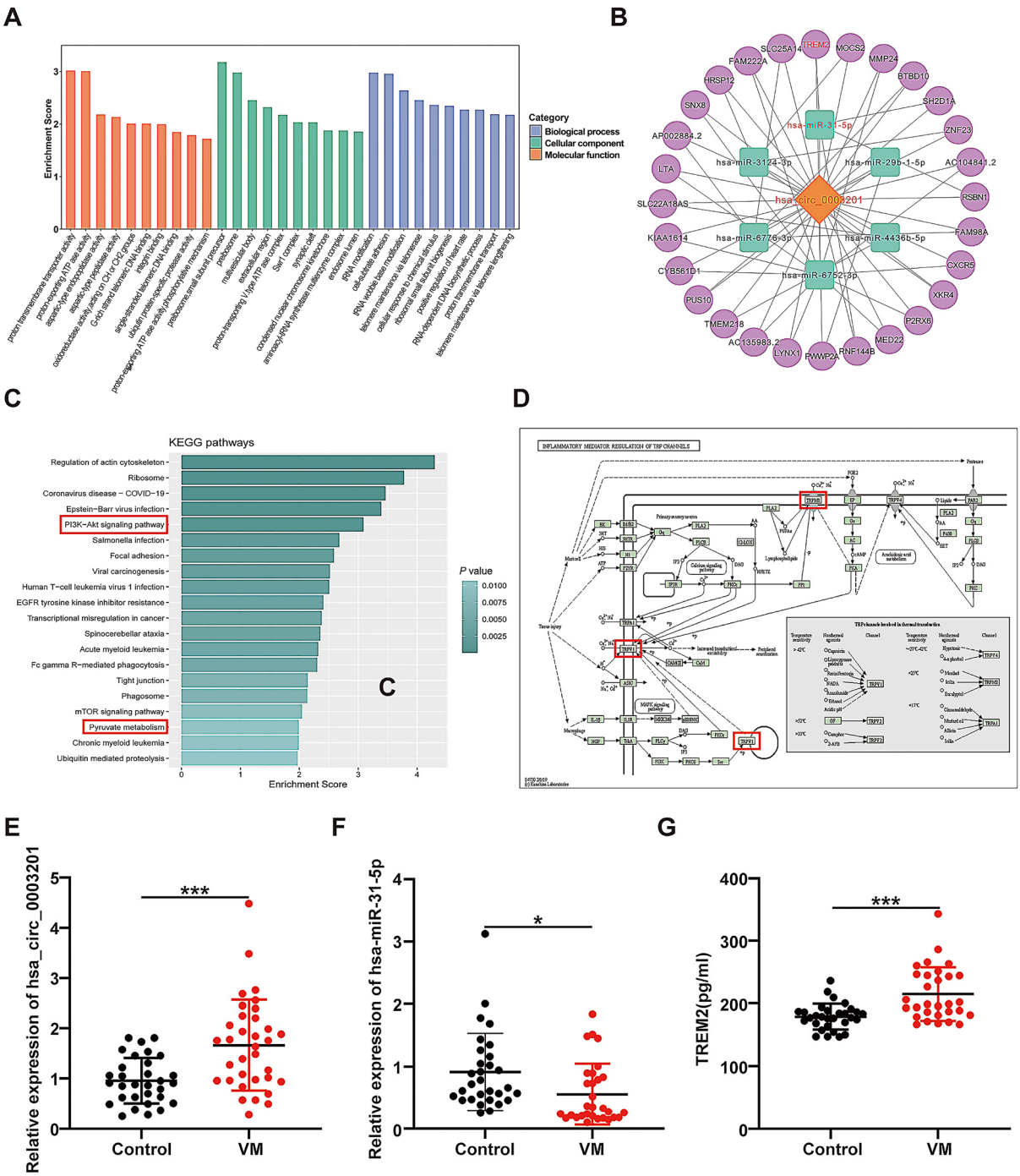

Fig. 2 Construction of the vestibular migraine (VM)-associated hsa_circ_0003201/miR-31-5p/triggering receptor expressed on myeloid cells 2 (TREM2) axis

(A) Gene ontology (GO) functional enrichment analysis of hsa_circ_0003201-related genes. (B) hsa_circ_0003201-based ceRNA network related to VM, with the key hsa_circ_0003201/miR-31-5p/TREM2 axis identified in this study highlighted in red. (C) Top 20 enriched pathways from Kyoto encyclopedia of genes and genomes (KEGG) pathway enrichment analysis, with the pathways relevant to this study highlighted in red. (D) The transient receptor potential (TRP) channel pathways (hsa04270, hsa04750). (E-F) Quantitative reverse transcription polymerase chain reaction (qRT-PCR) detection of hsa_circ_0003201 and hsa-miR-31-5p expression levels ($N = 30$/group). (G) Enzyme-linked immunosorbent assay (ELISA) analysis of TREM2 expression levels ($N = 30$/group). The data are presented as mean ± SD. Student's *t*-test (E-G). $^{*}P < 0.05$, $^{***}P < 0.001$.

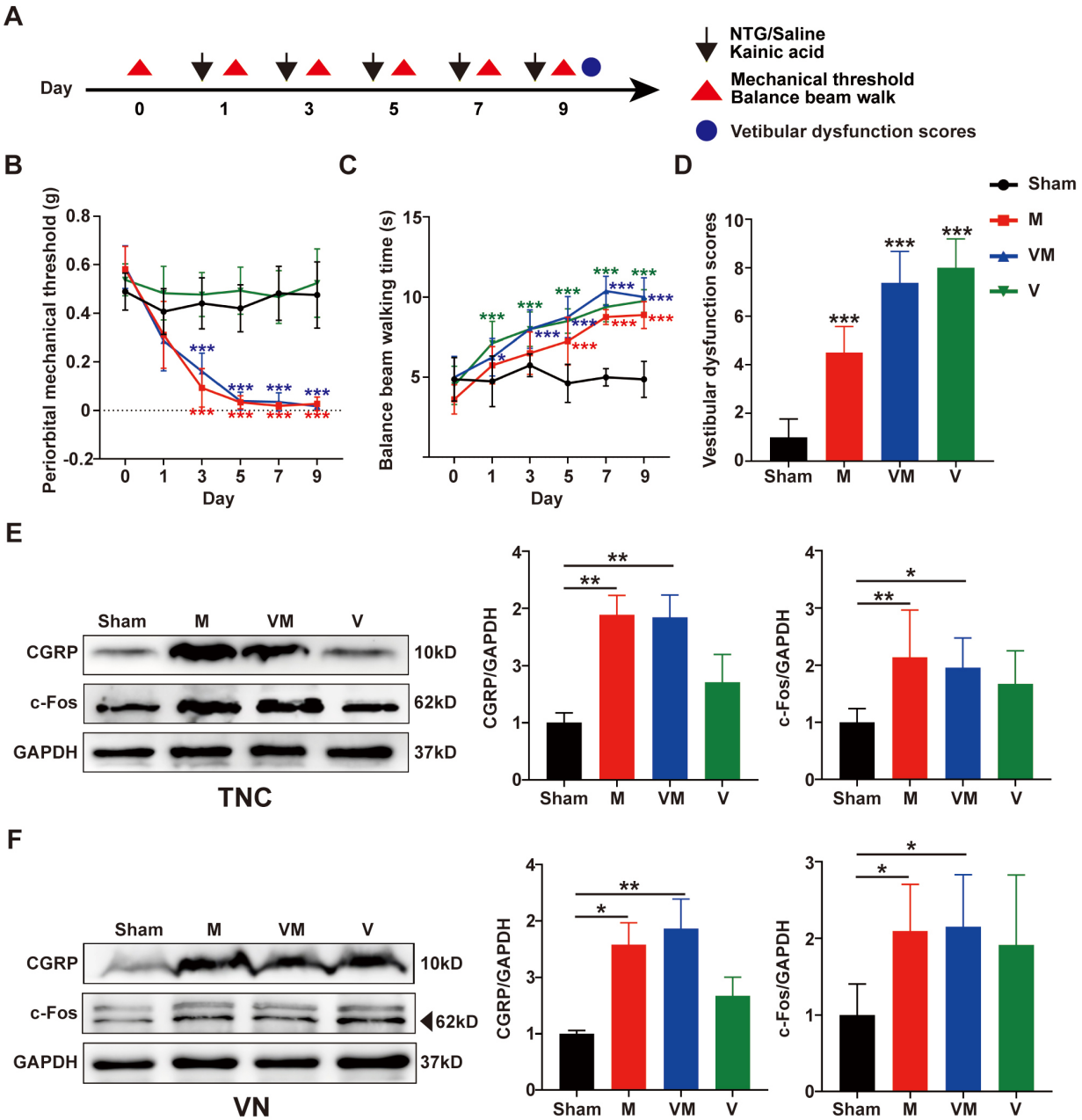

Fig. 3 Establishment of vestibular migraine (VM)-like mouse model

(A) Flowchart of mouse model induction and behavioral assessments. (B) The periorbital mechanical thresholds were assessed using von Frey filaments (N = 8/group). (C-D) Balance beam walking time and vestibular dysfunction tests of mice (N = 8/group). (E) Western blot analysis of calcitonin gene related peptide (CGRP) and c-Fos protein expression in the trigeminal nucleus caudalis (TNC) (N = 6/group). (F) CGRP and c-Fos protein levels in the vestibular nuclei (VN) analyzed by western blot (N = 6/group). The data are shown as mean ± SD. The P values were calculated using two-way analysis of variance (ANOVA) followed by Tukey's post hoc tests (B and C) and one-way ANOVA (D-F). $^{*}P < 0.05$, $^{**}P < 0.01$, $^{***}P < 0.001$. M, Migraine.

NTG combined with intratympanic KA (Fig. 3A). No baseline behavioral differences were observed. From day 3, NTG-treated M mice showed reduced periorbital mechanical thresholds (P = 0.0001, N = 8/group, two-way ANOVA with Tukey post hoc; Fig. 3B); from day 5, they exhibited prolonged balance-beam time (P = 0.0001; Fig. 3C) and higher vestibular-dysfunction scores (P = 0.0001, one-way ANOVA;

Fig. 3D), indicating hyperalgesia with mild vestibular impairment. In VM-like (NTG+KA) mice, balance-beam time was already prolonged on day 1 (P = 0.0455; Fig. 3C), followed by marked mechanical hypersensitivity from day 3 (P = 0.0001; Fig. 3B) and increased vestibular-dysfunction scores (P = 0.0001; Fig. 3D), consistent with combined vestibular dysfunction and hyperalgesia. In a KA-only (vertigo) group, vestibular impairment predominated without hyperalgesia (balance-beam time: P = 0.0002; vestibular score: P = 0.0001; Fig. 3C-D).

Because calcitonin gene related peptide (CGRP) promotes neuroinflammation and central sensitization[20] and c-Fos marks nociceptive activation[21], we quantified both in the trigeminal nucleus caudalis (TNC) and vestibular nuclei (VN). Western blot showed increased CGRP and c-Fos in TNC (CGRP: control *vs.* M P = 0.0043, control *vs.* VM P = 0.0051; c-Fos: control *vs.* M P = 0.0077, control *vs.* VM P = 0.0247; N = 6/group, one-way ANOVA; Fig. 3E) and VN (CGRP: control *vs.* M P = 0.0167, control *vs.* VM P = 0.0050; c-Fos: control *vs.* M P = 0.0289, control *vs.* VM P = 0.0210; Fig. 3F), indicating central sensitization with aberrant VN activation. These results validate that VM-like mice recapitulate key VM pathophysiology.

3.4 Reciprocal expression of TREM2 and miR-31-5p upon PI3K/AKT activation in TNC and VN of VM-like mice

To probe the hsa_circ_0003201/miR-31-5p/TREM2 axis *in vivo*, we measured miR-31-5p, TREM2, and PI3K/AKT signaling in TNC and VN. qRT-PCR showed reduced miR-31-5p in the VN of VM-like mice (control *vs.* M P = 0.9747; control *vs.* VM P = 0.0158; N = 6/group, one-way ANOVA; Fig. 4C), with a non-significant trend in TNC (control *vs.* M P = 0.9997; control *vs.* VM P = 0.1619; Fig. 4A). In contrast, TREM2 protein was increased in both TNC (control *vs.* M P = 0.1711; control *vs.* VM P = 0.0249; Fig. 4B) and VN (control *vs.* M P = 0.0846; control *vs.* VM P = 0.0038; Fig. 4D) of VM-like mice. Western blot indicated PI3K/AKT activation in M (PI3K: TNC P = 0.0309, VN P = 0.0158) and VM-like mice (PI3K: TNC P = 0.0349, VN P = 0.0023; p-AKT: TNC P = 0.0274, VN P = 0.0211; N = 6/group, one-way ANOVA; Fig. 4E-F). These data support involvement of the miR-31-5p/TREM2 axis and PI3K/AKT signaling in VM pathogenesis, with region-specific changes in VN.

3.5 Differentially expressed circRNAs between VM and M patients from cold regions

To compare molecular features of VM and M in cold regions, we profiled circRNAs in peripheral blood from 3 VM and 3 M patients. We identified 2308 differentially expressed circRNAs (FC ≥ 1.5, P < 0.05), including 1260 upregulated and 1048 downregulated (Fig. 5A). The top four up- and top four downregulated circRNAs were selected for follow-up (Fig. 5B); details are provided in Table 5. GO enrichment of mRNAs corresponding to these eight candidates implicated cell adhesion among biological processes; cellular components were enriched for membrane-associated structures, and molecular functions for calcium-ion binding (Fig. 5C). KEGG analysis highlighted regulation of the actin cytoskeleton and cell-adhesion molecules (Fig. 5D), suggesting distinct cytoskeletal and adhesion signaling differences between VM and M in cold-exposed populations.

4 Discussion

In this study, we identified a novel circRNA, hsa_circ_0003201, that is upregulated in the peripheral blood of VM patients living in cold regions. *In vivo* and *in vitro* evidence suggests that hsa_circ_0003201 may regulate the downstream miR-31-5p/TREM2 axis *via* a ceRNA mechanism, thereby contributing to VM onset and progression under cold-climate conditions. Pathway enrichment implicated cold-related TRP signaling, PI3K/AKT signaling, and pyruvate metabolism, indicating a potential integrative role for hsa_circ_0003201 in temperature-sensitive molecular networks relevant to VM.

VM likely arises from interactions between nociceptive and vestibular pathways. Extensive connections between the VN and other brainstem structures—such as the parabrachial nucleus, raphe nuclei, and locus coeruleus—may modulate trigeminovascular reflexes and pain-pathway sensitivity, with neuroinflammation as a key mediator. Depolarization of meningeal nociceptor terminals can trigger release of vasoactive neuropeptides (*e.g.*, CGRP, substance P), promoting neurogenic inflammation and activating microglia to secrete proinflammatory mediators that amplify central sensitization. Concurrent activation of the trigeminal-vestibular-cochlear reflex may increase plasma-protein extravasation in the inner ear, persistently sensitizing primary trigeminal afferents and eliciting VM symptoms[22-23]. Growing evidence indicates that circRNAs regulate neuroinflammatory processes[24]—for example, circ_0049472 attenuates Aβ-induced neuronal dysfunction *via* the miR-22-3p/PDE4A axis[25]; circ_0002590 derepresses NLRP1 by sponging miR-1184 to promote neuroinflammation in diabetic neuropathic pain[26]; and reduced circCDC14A in peripheral blood cells mitigates peri-infarct astrocyte activation and brain injury in acute ischemic stroke[27]. These observations support a role for circRNAs in VM pathogenesis through modulation of neuroinflammation.

We constructed a VM-associated hsa_circ_0003201/miR-31-5p/TREM2 axis and preliminarily validated it in clinical samples and a VM-like mouse model. miR-31-5p was significantly downregulated in patient blood and showed a decreasing trend in the TNC and VN of VM-like mice, suggesting a potential protective

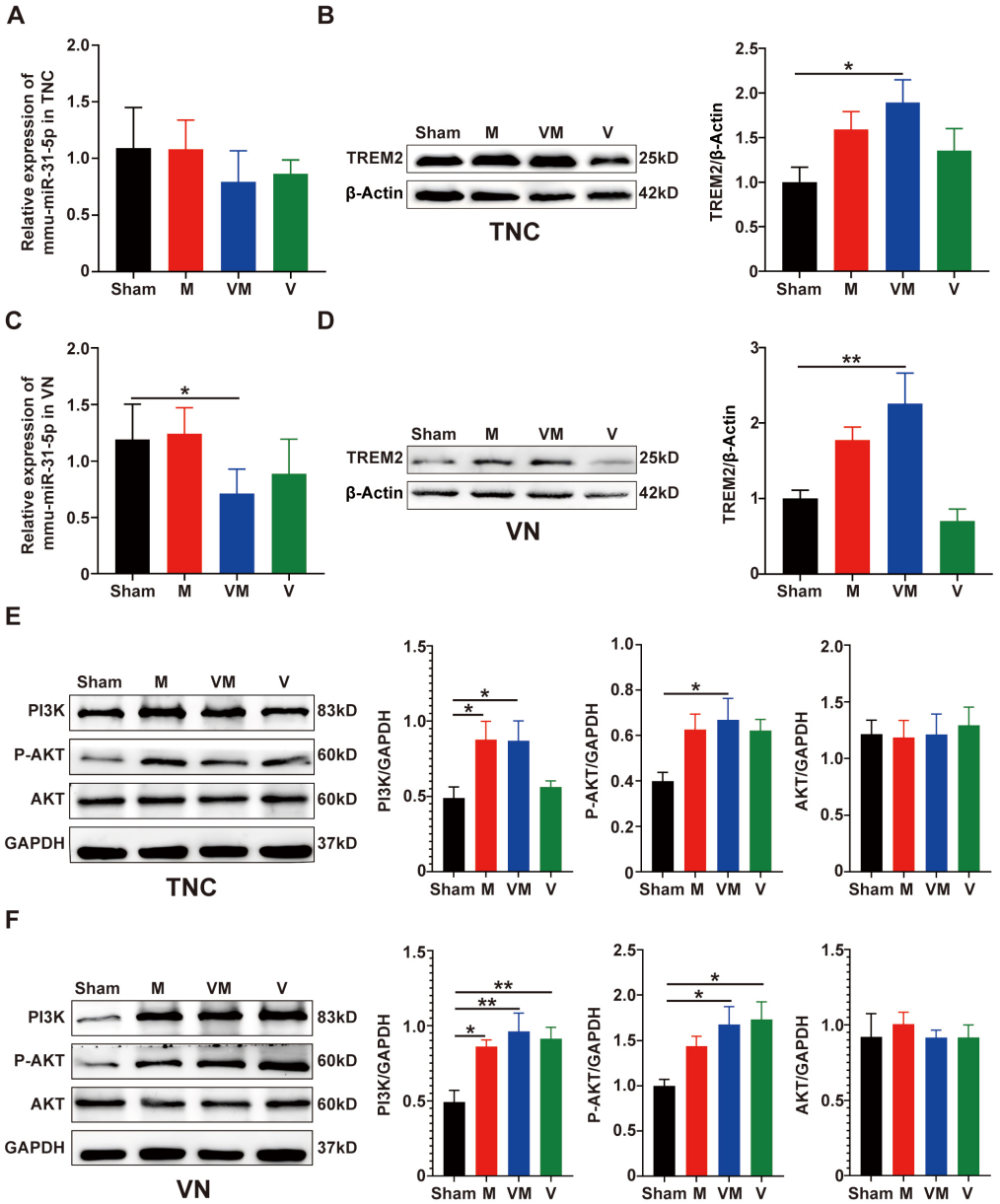

Fig. 4 Altered expression of triggering receptor expressed on myeloid cells 2 (TREM2) and miR-31-5p with activation of the phosphoinositide 3-kinase (PI3K)/protein kinase B (AKT) pathway in the trigeminal nucleus caudalis (TNC) and vestibular nuclei (VN) of vestibular migraine (VM)-like mice

(A) Quantitative reverse transcription polymerase chain reaction (qRT-PCR) analysis of mmu-miR-31-5p expression in the TNC. (B) Western blot analysis of TREM2 in the TNC of each group. (C) qRT-PCR validation of mmu-miR-31-5p in VN. (D) TREM2 protein levels in the VN analyzed by western blot. (E-F) Western blot analysis of PI3K/AKT pathway proteins in the TNC and VN of mice. $N = 6$/group. The data are presented as mean ± SD. The P values were calculated using one-way analysis of variance (ANOVA) (A-F). $^{*}P < 0.05$, $^{**}P < 0.01$. M, Migraine.

role. Prior studies align with this interpretation: miR-31-5p is reduced in chronic inflammatory demyelinating polyneuropathy, with IVIg treatment associated with its restoration[28]; in a chronic constriction injury model, miR-31-5p suppresses TRAF6 and lowers TNF-α, IL-6, and IL-1β, alleviating pain[29]; and miR-31-5p modulates PI3K/AKT signaling in multiple tumors[30-31]. Taken together, miR-31-5p appears to be closely linked to neuroinflammatory regulation, potentially *via* PI3K/AKT.

TREM2 is a microglial transmembrane receptor that mediates

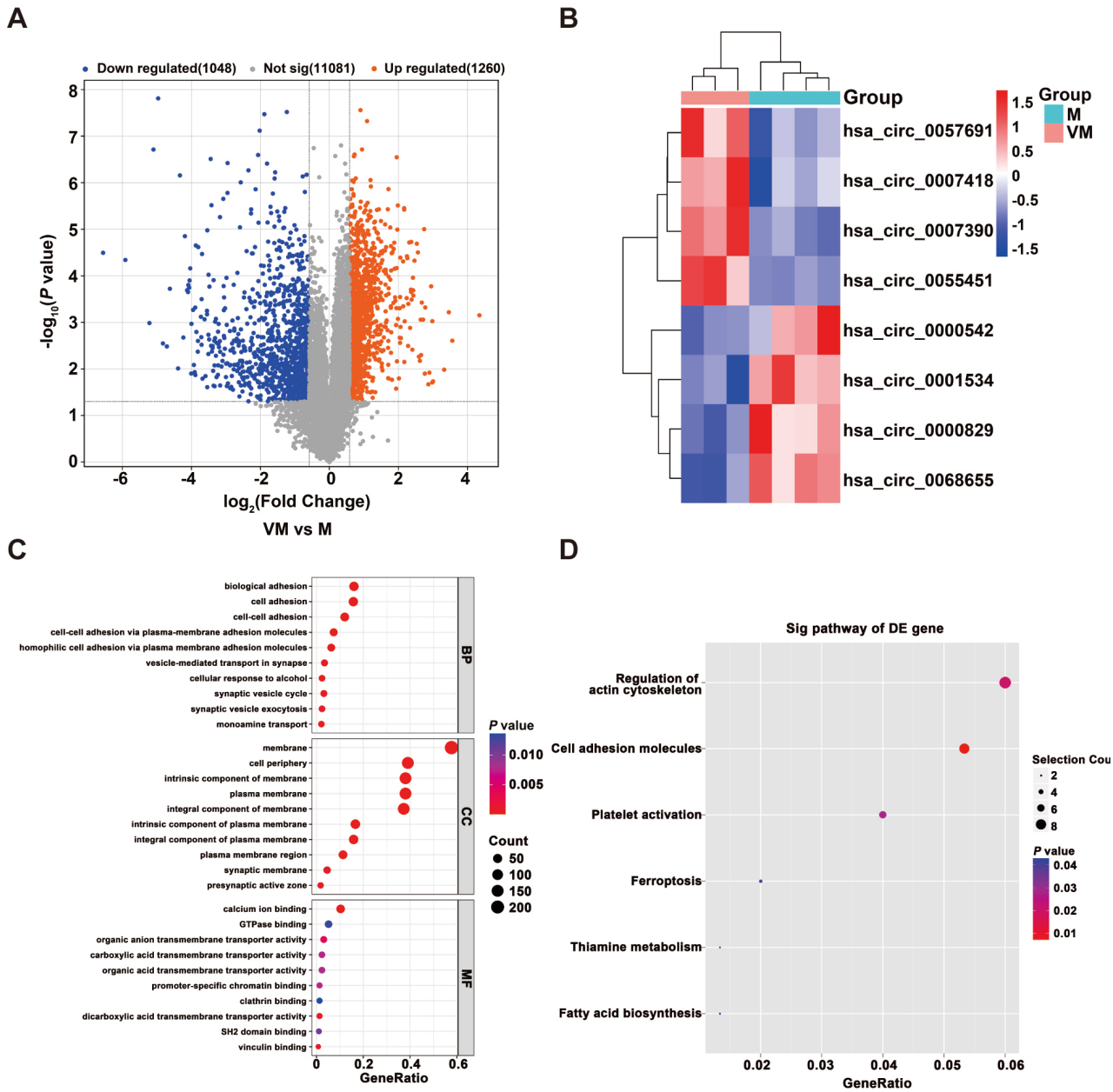

Fig. 5 Screening of differentially expressed circRNAs in vestibular migraine (VM) and Migraine (M) patients

(A) Volcano plot of differentially expressed circRNAs between VM and M patients. (B) Top 4 upregulated and top 4 downregulated circRNAs. (C-D) Gene ontology (GO) functional and Kyoto encyclopedia of genes and genomes (KEGG) pathway enrichment analysis of differentially expressed circRNAs in VM and M patients.

intracellular tyrosine phosphorylation, regulates immune responses, and controls phagocytosis[32]. TREM2 dysfunction exacerbates neurodegenerative disease pathology (*e.g.*, impaired microglial clearance of Aβ in AD), and peripheral immune effects include promotion of Th2/Th17 differentiation[33]. In a chronic migraine model induced by repeated nitroglycerin, TREM2 drove microglial activation in the TNC *via* the SYK cascade, triggering NLRP3 inflammasome activation and central sensitization[34]. Although direct links to vestibular dysfunction remain to be established, our data—elevated TREM2 in patient blood and in TNC/VN of VM-like mice—support a pathogenic role. Additional studies show that TREM2 modulates neuroinflammation and apoptosis *via* PI3K/AKT after intracerebral hemorrhage[35] and attenuates microglia-mediated inflammation to improve postop-

Table 5 Top 4 upregulated and top 4 downregulated circRNAs between vestibular migraine (VM) and Migraine (M) patients

Circbase ID	Chrom	*P* value	Fold change (abs)	Regulation	circRNA_type	Gene symbol
hsa_circ_0057691	Chr2	0.021791	1.976748	Up	Exonic	SATB2
hsa_circ_0007390	Chr15	0.000234	1.901624	Up	Exonic	NPTN
hsa_circ_0055451	Chr2	0.007965	1.846619	Up	Exonic	ST3GAL5
hsa_circ_0007418	chr1	0.005496	1.783638	Up	Exonic	ZBTB40
hsa_circ_0068655	Chr3	0.001609	14.468478	Down	Exonic	UBXN7
hsa_circ_0000542	Chr14	0.017122	3.332816	Down	Exonic	ARID4A
hsa_circ_0001534	Chr5	0.001058	1.638913	Down	Exonic	FAM13B
hsa_circ_0000829	Chr18	0.013600	1.510387	Down	Exonic	SPIRE1

erative cognition through PI3K/AKT regulation[36]. Collectively, these findings support the hypothesis that the hsa_circ_0003201/miR-31-5p/TREM2 axis contributes to VM pathogenesis by regulating microglial activation and inflammatory signaling through PI3K/AKT, thereby facilitating central sensitization.

Cold stimuli can activate peripheral TRP channels and depolarize neuronal membranes, transmitting excitatory signals centrally. TRPA1, expressed in subsets of primary sensory neurons (including trigeminal ganglia), can trigger CGRP and substance P release and neurogenic inflammation; TRPA1 antagonists have thus been proposed for neuropathic pain and migraine[37]. TRPM8, activated below ~28 °C, drives Ca^{2+} influx and enhances transmitter release[38]; its expression in meningeal CGRP afferents suggests that activation/sensitization may sustain hyperexcitability and transmitter release[39]. Environmental and stress-related inputs interface with these channels and PI3K/AKT: ozone exposure activates TRPA1 and induces ferroptosis/mitochondrial dysfunction *via* PI3K/AKT/OPA1[40], and acute stress can activate PI3K/AKT *via* glucocorticoid receptors to enhance TRPM8 in dorsal root ganglia, contributing to visceral hypersensitivity[41]. Cold may also influence migraine through metabolic routes: dysregulated glycolysis/gluconeogenesis—particularly pyruvate handling—is associated with attacks, and reactive hypoglycemia (*e.g.*, after fasting/high-carbohydrate intake) is a recognized trigger whose incidence rises in cold environments[42]. Consistent with these connections, our KEGG results for hsa_circ_0003201-associated transcripts clustered in PI3K/AKT, pyruvate metabolism, and TRP pathways. We therefore hypothesize that, under cold stress, the hsa_circ_0003201/miR-31-5p/TREM2 axis promotes VM *via* coordinated modulation of PI3K/AKT, pyruvate metabolism, and TRP signaling; detailed mechanistic testing will be pursued in future work.

Since the 2018 ICHD-3, definite vestibular migraine (dVM) has been listed in the appendix of migraine-related disorders to facilitate research[14]. While migraine and VM share mechanisms (genetic susceptibility, neurotransmitter imbalance, abnormal brain networks)[4], VM is distinguished by prominent vestibular symptoms, implying additional regulatory layers. Our previous work identified abnormalities in a vestibulocerebellum GABAergic-VN glutamatergic-Sp5C astrocytic circuit linking vestibular signals to pain processing, supporting VM-specific circuitry[43]. Here, comparison of VM and migraine circRNA profiles in cold-region patients identified 2308 differentially expressed circRNAs, further validation will be required to define VM-specific molecular features.

This study has limitations. First, although circRNAs are relatively conserved (~28% sequence/expression similarity between humans and mice, particularly in brain)[44], a direct mouse homolog of hsa_circ_0003201 was not identified, precluding one-to-one mechanistic testing in our VM-like model. Second, the discovery microarray and clinical validation cohorts were modest in size, and the causal ordering and functional contribution of the hsa_circ_0003201/miR-31-5p/TREM2 axis remain to be established. Future work will delineate this axis and its hierarchy using larger clinical sets and cellular systems. Third, despite attempts, a cold-induced VM-like mouse model did not yield robust behavioral changes; further optimization of cold-stimulation paradigms is needed to clarify hsa_circ_0003201 function in cold-region VM.

5 Conclusion

In summary, among long-term residents of Heilongjiang Province, hsa_circ_0003201 was significantly upregulated in VM and, together with clinical and animal data, supports a working model in which the hsa_circ_0003201/miR-31-5p/TREM2 axis contributes to VM pathogenesis *via* PI3K/AKT, pyruvate metabolism, and TRP signaling. Comparative circRNA profiling between cold-region VM and migraine suggests that VM may exhibit a distinct molecular signature rather than representing merely a migraine subtype. Further validation and mechanistic studies are warranted to substantiate these conclusions and to explore translational opportunities.

Acknowledgements

Not applicable.

Research ethics

This study received approval from the Ethics Committee of the First Affiliated Hospital of Harbin Medical University (IRB-AF/SC-12/03.0), and written informed consent was obtained from all participants. All animal experiments were conducted in accordance with protocols approved by the Institutional Animal Care and Use Committee of the same institution (2022-K98).

Informed consent

All participants provided written informed consent prior to enrollment.

Author contributions

Study conception and design by Pan Y H, Lin J H; Experimental work and data collection by Chen Q H; Clinical sample collection by Yu Q J; Bioinformatics and statistical analysis by Zhai Q L; Manuscript drafting: Chen Q H, Zhai Q L, Yu Q J; and Critical revision and final approval by Pan Y H, Lin J H. All authors read and approved the final manuscript.

Use of large language models, AI and machine learning tools

No large language models, AI or machine learning tool was used for any part of the present study.

Conflict of interests

The authors declare no competing interests.

Research funding

This study was supported by General Program of National Natural Science Foundation of China (No. 82071549, 82371483); Key Research & Development Program of Heilongjiang (No. 2023ZX06C02); and Youth Foundation of the first Affiliated Hospital of Harbin Medical University (No. 2024YQ22).

Data availability

The data generated in this study are available from the corresponding author upon reasonable request.

References

[1] Dong L, Dong W, Jin Y, *et al.* The global burden of migraine: A 30-year trend review and future projections by age, sex, country, and region. Pain Ther, 2025; 14(1): 297-315.
[2] GBD 2016 Neurology Collaborators. Global, regional, and national burden of neurological disorders, 1990-2016: A systematic analysis for the Global Burden of Disease Study 2016. Lancet Neurol, 2019; 18(5): 459-480.
[3] Formeister E J, Rizk H G, Kohn M A, *et al.* The epidemiology of vestibular migraine: A population-based survey study. Otol Neurotol, 2018; 39(8): 1037-1044.
[4] Furman J M, Marcus D A, Balaban C D. Vestibular migraine: Clinical aspects and pathophysiology. Lancet Neurol, 2013; 12(7): 706-715.
[5] Ye S, Gao Y, Lin Y, *et al.* Ambient nitrogen dioxide, temperature exposure, and migraine incidence: A large prospective cohort study. Headache, 2025; 65(8): 40859714.
[6] Li W, Bertisch S M, Mostofsky E, *et al.* Weather, ambient air pollution, and risk of migraine headache onset among patients with migraine. Environ Int, 2019; 132: 105100.
[7] Scheidt J, Koppe C, Rill S, *et al.* Influence of temperature changes on migraine occurrence in Germany. Int J Biometeorol, 2013; 57(4): 649-654.
[8] Zhang J, Luo Z, Zheng Y, *et al.* CircRNA as an Achilles heel of cancer: Characterization, biomarker and therapeutic modalities. J Transl Med, 2024; 22(1): 752.
[9] Misir S, Wu N, Yang B B. Specific expression and functions of circular RNAs. Cell Death Differ, 2022; 29(3): 481-491.
[10] Yang L, Han B, Zhang Z, *et al.* Extracellular vesicle-mediated delivery of circular RNA SCMH1 promotes functional recovery in rodent and nonhuman primate ischemic stroke models. Circulation, 2020; 142(6): 556-574.
[11] García-Domínguez M. Role of ncRNAs in the development of chronic pain. Noncoding RNA, 2025; 11(4): 51.
[12] Lin J, Shi S, Chen Q, *et al.* Differential expression and bioinformatic analysis of the circRNA expression in migraine patients. Biomed Res Int, 2020; 2020: 4710780.
[13] Song B, Fu J, Cheng J, *et al.* Circular RNA circFat3 as a biomarker for construction of postmortem interval Estimation models in mouse brain tissues at multiple temperatures. Sci Rep, 2025; 15(1): 21577.
[14] Headache Classification Committee of the International Headache Society (IHS). The International Classification of Headache Disorders, 3rd edition (beta version). Cephalalgia, 2013; 33(9): 629-808.
[15] Chen H, Tang X, Li J, *et al.* IL-17 crosses the blood-brain barrier to trigger neuroinflammation: a novel mechanism in nitroglycerin-induced chronic migraine. J Headache Pain, 2022; 23(1): 1.
[16] Gaboyard-Niay S, Travo C, Saleur A, *et al.* Correlation between afferent rearrangements and behavioral deficits after local excitotoxic insult in the mammalian vestibule: A rat model of vertigo symptoms. Dis Model Mech, 2016; 9(10): 1181-1192.
[17] Chaplan S R, Bach F W, Pogrel J W, *et al.* Quantitative assessment of tactile allodynia in the rat paw. J Neurosci Methods, 1994; 53(1): 55-63.
[18] Cohen J M, Bigal M E, Newman L C. Migraine and vestibular symptoms-identifying clinical features that predict vestibular migraine.

Headache, 2011; 51(9): 1393-1397.
[19] Saldaña-Ruíz S, Soler-Martín C, Llorens J. Role of CYP2E1-mediated metabolism in the acute and vestibular toxicities of nineteen nitriles in the mouse. Toxicol Lett, 2012; 208(2): 125-132.
[20] Li H, Huang Y, Chen Q, *et al.* Effect of activated autophagy on an animal model of vestibular migraine-like attacks. Exp Neurol, 2025; 392: 115366.
[21] Wen Q, Wang Y, Pan Q, *et al*. MicroRNA-155-5p promotes neuroinflammation and central sensitization *via* inhibiting SIRT1 in a nitroglycerin-induced chronic migraine mouse model. J Neuroinflammation, 2021; 18(1): 287.
[22] Ashina M. Migraine. N Engl J Med, 2020; 383(19): 1866-1876.
[23] Espinosa-Sanchez J M, Lopez-Escamez J A. New insights into pathophysiology of vestibular migraine. Front Neurol, 2015; 6: 12.
[24] Muhammed T M, Jasim S A, Uthirapathy S, *et al.* CircRNA-based therapeutics: A new frontier in neuroinflammation treatment. Mol Neurobiol, 2025; Published online: 40745517.
[25] Chen J, Xiao S, Cui X, *et al.* Circ_0049472 downregulation relieves Amyloid-β-induced neuronal injury by modulating PDE4A expression *via* targeting miR-22-3p in Alzheimer's disease. Metab Brain Dis, 2025; 40(7): 252.
[26] Liu Q, Chen M, Cai X, *et al*. Role of circ_0002590 in neuroinflammation *via* the miR-1184/NLRP1 axis in painful diabetic neuropathy. Exp Clin Endocrinol Diabetes, 2025; 133(8): 415-424.
[27] Zuo L, Xie J, Liu Y, *et al.* Down-regulation of circular RNA CDC14A peripherally ameliorates brain injury in acute phase of ischemic stroke. J Neuroinflammation, 2021; 18(1): 283.
[28] Dziadkowiak E, Baczyńska D, Wieczorek M, *et al.* MiR-31-5p as a potential circulating biomarker and tracer of clinical improvement for chronic inflammatory demyelinating polyneuropathy. Oxid Med Cell Longev, 2023; 2023: 2305163.
[29] Liu Y, Wang L, Zhou C, *et al*. MiR-31-5p regulates the neuroinflammatory response *via* TRAF6 in neuropathic pain. Biol Direct, 2024; 19(1): 10.
[30] Zhao J, Xu H, Duan Z, *et al.* MiR-31-5p regulates 14-3-3 ε to inhibit prostate cancer 22RV1 cell survival and proliferation *via* PI3K/AKT/Bcl-2 signaling pathway. Cancer Manag Res, 2020; 12: 6679-6694.
[31] Wang W, Tang L, Li Q, *et al.* Overexpression of miR-31-5p inhibits human chordoma cells proliferation and invasion by targeting the oncogene c-Met through suppression of AKT/PI3K signaling pathway. Int J Clin Exp Pathol, 2017; 10(7): 8000-8009.
[32] Wang Y, Cella M, Mallinson K, *et al.* TREM2 lipid sensing sustains the microglial response in an Alzheimer's disease model. Cell, 2015; 160(6): 1061-1071.
[33] Bayraktaroglu I, Ortí-Casañ N, Van Dam D, *et al*. Systemic inflammation as a central player in the initiation and development of Alzheimer's disease. Immun Ageing, 2025; 22(1): 33.
[34] Fan Z, Su D, Li Z C, *et al.* Metformin attenuates central sensitization by regulating neuroinflammation through the TREM2-SYK signaling pathway in a mouse model of chronic migraine. J Neuroinflammation, 2024; 21(1): 318.
[35] Chen S, Peng J, Sherchan P, *et al.* TREM2 activation attenuates neuroinflammation and neuronal apoptosis *via* PI3K/Akt pathway after intracerebral hemorrhage in mice. J Neuroinflammation, 2020; 17(1): 168.
[36] Han X, Cheng X, Xu J, *et al*. Activation of TREM2 attenuates neuroinflammation *via* PI3K/Akt signaling pathway to improve postoperative cognitive dysfunction in mice. Neuropharmacology, 2022; 219: 109231.
[37]N assini R, Materazzi S, Benemei S, *et al.* The TRPA1 channel in inflammatory and neuropathic pain and migraine. Rev Physiol Biochem Pharmacol, 2014; 167: 1-43.
[38] Yue L, Xu H. TRP channels in health and disease at a glance. J Cell Sci, 2021; 134(13): jcs258372.
[39] Strassman A, Mason P, Moskowitz M, *et al.* Response of brainstem trigeminal neurons to electrical stimulation of the dura. Brain Res, 1986; 379(2): 242-250.
[40] Weng J, Liu Q, Li C, *et al.* TRPA1-PI3K/Akt-OPA1-ferroptosis axis in ozone-induced bronchial epithelial cell and lung injury. Sci Total Environ, 2024; 918: 170668.
[41] Luo Q Q, Wang B, Chen X, *et al*. Acute stress induces visceral hypersensitivity *via* glucocorticoid receptor-mediated membrane insertion of TRPM8: Involvement of a non-receptor tyrosine kinase Pyk2. Neurogastroenterol Motil, 2020; 32(10): 1514-1528.
[42] Kelbert J, Tobin J A. The effect of ambient temperature on migraine disease: A scoping review. Brain Behav, 2025; 15(8): e70708.
[43] Zhai Q, Chen Q, Zhang N, *et al.* Exploring vestibulocerebellum-vestibular nuclei-spinal trigeminal nucleus causals communication and
[44] TRPV2 ion channel in a mouse model of vestibular migraine. J Headache Pain, 2025; 26(1): 47.
Hanan M, Soreq H, Kadener S. CircRNAs in the brain. RNA Biol, 2017; 14(8): 1028-1034.